HHS Public Access

Author manuscript

Cancer Res. Author manuscript; available in PMC 2020 July 01.

Published in final edited form as:

Cancer Res. 2020 January 01; 80(1): 57–68. doi:10.1158/0008-5472.CAN-19-1676.

Heparanase and chemotherapy synergize to drive macrophage activation and enhance tumor growth

Udayan Bhattacharya[1], **Lilach Gutter-Kapon**[1], **Tal Kan**[1,2], **Ilanit Boyango**[1], **Uri Barash**[1], **Shi-Ming Yang**[3], **JingJing Liu**[3], **Miriam Gross-Cohen**[1], **Ralph D. Sanderson**[4], **Yuval Shaked**[1,2], **Neta Ilan**[1], **Israel Vlodavsky**[1,*]

[1]Technion integrated cancer center (TICC), Rappaport Faculty of Medicine, Technion, Haifa, Israel

[2]Department of Cell Biology and Cancer Science, Rappaport Faculty of Medicine, Technion, Haifa, Israel

[3]Department of Gastroenterology, Xinqiao Hospital, Third Military Medical University, Chongqing 400037, China

[4]University of Alabama at Birmingham, Department of Pathology, Birmingham, AL 35294, USA

Abstract

The emerging role of heparanase in tumor initiation, growth, metastasis, and chemoresistance is well recognized, encouraging the development of heparanase inhibitors as anticancer drugs. Unlike the function of heparanase in cancer cells, little attention has been given to heparanase contributed by cells composing the tumor microenvironment. Here, we focused on the cross-talk between macrophages, chemotherapy, and heparanase and the combined effect on tumor progression. Macrophages were markedly activated by chemotherapeutics paclitaxel (PCT) and cisplatin, evidenced by increased expression of pro-inflammatory cytokines, supporting recent studies indicating that chemotherapy may promote rather than suppress tumor re-growth and spread. Strikingly, cytokine induction by chemotherapy was not observed in macrophages isolated from heparanase-knockout mice, suggesting macrophage activation by chemotherapy is heparanase-dependent. PCT-treated macrophages enhanced the growth of lewis lung carcinoma tumors which was attenuated by a CXCR2 inhibitor. Mechanistically, PCT and cisplatin activated methylation of histone H3 on lysine 4 (H3K4) in wild-type but not heparanase-knockout macrophages. Furthermore, the H3K4 presenter WDR5 functioned as a molecular determinant that mediated cytokine induction by PCT. This epigenetic, heparanase-dependent host-response mechanism adds a new perspective to the tumor-promoting functions of chemotherapy, and offers new treatment modalities to optimize chemotherapeutics.

Precise:

Chemotherapy-treated macrophages are activated to produce pro-inflammatory cytokines, which is blunted in the absence of heparanase

*To whom correspondence should be addressed: Israel Vlodavsky, Technion integrated cancer center (TICC), Rappaport Faculty of Medicine, Technion, P. O. Box 9649, Haifa 31096, Israel, Tel. 972-4-8295410; Fax. 972-4-8523947, Vlodavsk@mail.huji.ac.il.

Conflict of Interest: The authors have no potential conflict of interest to declare.

Keywords

Heparanase; macrophages; paclitaxel; tumor growth; histone methylation; WDR5

Introduction

Heparanase is an endo-β-D-glucuronidase capable of cleaving heparan sulfate (HS) side chains at a limited number of sites (1, 2). Heparanase activity is highly implicated in the metastatic potential of tumor-derived cells, a consequence of remodeling of the extracellular matrix (ECM) underlying epithelial and endothelial cells (2-4). Similar considerations tie heparanase activity with neovascularization, inflammation, and autoimmunity, facilitating the motility of vascular endothelial cells and activated cells of the immune system (5, 6). Compelling evidence gathered in the last two decades revealed that heparanase expression is up-regulated in an increasing number of human carcinomas, sarcomas, and hematological malignancies. Most often, heparanase induction correlated with increased tumor metastasis and shorter survival of cancer patients (6-9), thus providing strong clinical support for the pro-tumorigenic function of the enzyme and encouraging the development of heparanase inhibitors as anti-cancer drugs (10, 11).

While novel therapeutics modalities are developed and implemented successfully (i.e., immune checkpoint inhibitors), chemotherapy is still the leading and most powerful treatment for cancer patients. Recent studies, nonetheless, suggest that chemotherapy, in addition to its cytotoxic effects on tumor cells, can support tumor re-growth and spread (12). For example, mice that had been pre-treated with paclitaxel (PCT) or cisplatin before intravenous injection of tumor cells succumbed to metastatic disease earlier than control mice (12-14). Similarly, fibrosarcoma cells intravenously injected into C57Bl/6 mice that had been previously treated with bleomycin developed increased pulmonary metastases (15). Importantly, this paradoxical effect of chemotherapy that emerged from preclinical research is likely to have human relevance (16).

Given the established role of heparanase in tumor metastasis, we examined whether increased metastasis by chemotherapy is due to induction of heparanase. This notion emerged from previous reports showing that heparanase expression is increased substantially in myeloma patients and cells treated with chemotherapy (17, 18).

Materials and methods

Cells and cell culture.

Human U87 glioma, MSTO-211H and NCI-2052H mesothelioma, and SGC7901 gastric carcinoma cells have been described previously (19-21). The cell lines were authenticated in June 2018 by the short tandem repeat (STR) profile of 15 loci plus amelogenin for sex determination (X or XY) method according to the manufacturer's (Promega) instructions, as described (19, 20). Lewis lung carcinoma (LLC) and J774 murine macrophage cells have been described previously (22). Mouse peritoneal monocytes/macrophages (MPM) were harvested from the peritoneal fluid of WT or Hpa-KO C57BL/6 mice three days after

intraperitoneal injection of thioglycolate (3 ml; 40 mg/ml), essentially as described (22). Peritoneal exudate cells (5×10^6) were plated in 60-mm dish for 24 hours and cultured in Dulbecco's Modified Eagle's Medium (DMEM) supplemented with glutamine, pyruvate, antibiotics and 10% fetal calf serum in a humidified atmosphere containing 5% CO_2 at 37°C. Non-adherent cells were removed after 24 hours by washing and the cells remaining attached were considered as macrophages (22). Macrophages were then grown for additional 24 hours in 2% FCS followed by treatment with PCT, Cisplatin, or doxorubicin for the times and concentrations indicated. Cells were free of mycoplasma contamination.

Cell lysates and protein blotting.

Preparation of cell lysates and protein blotting were carried out essentially as described (22).

Heparanase enzymatic activity.

Preparation of ECM-coated 35mm dishes and determination of heparanase activity were performed as described in detail elsewhere (23). Briefly, to evaluate heparanase activity in live cells, cultures of U87 glioma cells were left untrtaed or were treated with the indicated concentration of Hep1001 for 18h. Cells were then washed and lysed by three freeze/thaw cycles. The resulting cell extracts were incubated (18 h, 37°C, pH 5.8) with ^{35}S-labeled ECM, in a 35 mm dish. The incubation medium was then collected and subjected to gel filtration on a Sepharose CL-6B column. Fractions of 0.2 ml are eluted with PBS and measured for their radioactivity in a β-scintillation counter. Degradation fragments of HS side chains are eluted at $0.5< K_{av}<0.8$ (fractions 15-30). Hep1001 was similarly incubated with recombinant active heparanase (200 ng) for 5h at 37°C and heparanase activity was evaluated as above (22, 24).

Real-time PCR analyses.

Total RNA was extracted with TRIzol (Sigma), and RNA (1 μg) was amplified using the one-step PCR amplification kit, according to the manufacturer's (ABgene, Epsom, UK) instructions. The PCR primer sets utilized in this study are listed in Suppl. Table 1. Cytokines expression was normalized to actin. Data are expressed as the mean level of expression normalized to actin, and data represent the mean±SEM of triplicate samples; results are representative of three independent experiments (22).

Antibodies and reagents.

Rat anti-mouse F4/80 antibody was purchased from Serotec; Rat anti-mouse CD31 was purchased from Dianova (Hamburg, Germany). Anti-actin and anti-smooth muscle actin (SMA) monoclonal antibodies were purchased from Sigma (St. Louis, MO). Antibodies directed against phopsho-AMPK alpha, phospho-p38 and phospho-JNK, histone H3 and H3K4-di (H3K4me2) and -tri (H3K4Me3) methylation, H3K27 tri-methylation and acetylated H2BK5 were purchased from Cell Signaling Technology (Beverly, MA). Anti-WDR5, anti-BiP, and anti-Ly6g antibodies were purchased from Abcam (Cambridge, UK). The selective inhibitors of LSD1 (GSK-2879552), WDR5 (OICR-9429), MKL1 (CCG-203971), CXCR2 (SB 225002), p38 (SB208530), and JNK (sp600125) were purchased from ApexBio (Boston, MA) and were dissolved in DMSO as stock solutions.

DMSO (Sigma D2438) was added to the cell culture medium as control. The heparanase inhibitors H1001 and PG545 were kindly provided by HepaRx Ltd (Ness-Ziona, Israel) and Zucero Therapeutics (Darra, Queensland, Australia), respectively. Mouse CXCL2/MIP-2 Quantikine ELISA kit was purchased from R&D Systems (Minneapolis, MN). The MyD88 peptide inhibitory set was purchased from Novus Biologicals (Centennial, CO). Latent heparanase was purified from medium conditioned by CHO cells overexpressing heparanase essentially as described (25) and was added to cell cultures at 1 μg/ml.

Cell migration.

Migration assay was performed using modified Boyden chambers with polycarbonate Nucleopore membrane (Corning, Corning, NY). Filters (6.5 mm in diameter, 8 μm pore-size) were coated with fibronectin (30 μl; 10 μg/ml). WT macrophages (2×10^5) in 100 μl of serum-free medium were seeded in triplicate on the upper part of each chamber, and the lower compartment was filled with 600 μl medium conditioned by WT or KO macrophages that were not treated or treated with PCT for 24 h. After incubation for 24 h at 37°C in a 5% CO_2 incubator, non-invading cells on the upper surface of the filter were wiped with a cotton swab, and migrated cells on the lower surface of the filter were fixed, stained with 0.5% crystal violet (Sigma) and counted by examination of at least five microscopic fields, as described (26).

Tumorigenicity and immunohistochemistry.

Co-injection of LLC and macrophages was carried out essentially as described (22). Briefly, LLC cells were detached with trypsin/EDTA, washed with PBS, and brought to a concentration of 4×10^6 cells/ml. Control (untreated) and PCT-treated macrophages were mixed with LLC cells at a ratio of 1:1 and cell suspension (8×10^5/0.1 ml) was inoculated subcutaneously at the right flank of 6-8 weeks old WT (Envigo RMS LTD, Jerusalem, Israel) and Hpa-KO (in-house bred) C57Bl/6 mice. Xenograft size was determined by externally measuring tumors in 2 dimensions using a caliper. At the end of the experiment, mice were sacrificed, and tumors were removed and weighed. RNA was extracted from a small portion of the tumor, and the remaining portion was fixed in formalin. Paraffin-embedded 5μm sections were subjected to immunostaining applying the indicated antibodies using the Envision kit according to the manufacturer's (Dako) instructions, as described (22). Pictures were captured with a Nikon Digital Sight camera attached to Nikon Eclipse microscope. Immunofluorescent staining was performed on methanol-fixed macrophages essentially as described (27). For Matrigel experiments, control and PCT-treated macrophages were prepared similarly, detached, and resuspended in ice-cold Matrigel (3×10^6/ml). 0.5 ml of Matrigel-cell suspension were implanted subcutaneously in WT mice (n=6) and Matrigel plugs were excised two weeks later. Matrigel plugs were fixed in formalin, embedded in paraffin and five-micron sections were subjected to histological evaluation and immunostaining. Matrigel was also implanted in mice without cells as control. All experiments were performed in accordance with the Technion's Institutional Animal Care and Use Committee (IL-049-03-2017; OPRR-A5026-01).

Flow cytometry.

Control and PCT/cisplatin-treated macrophages were subjected to flow cytometry essentially as described previously (22, 28). The antibodies utilized for flow cytometry analyses are listed in Suppl. Table 2.

Statistics.

Results are shown as means ±SE. GraphPad Instat software was used for statistical analysis. The differences between the control and the treatment groups were determined by Student's t-Test/ one-way ANOVA, and post-test analyses were done using Dunnett's/ Bonferroni multiple comparison test. A value of $p \leq 0.05$ was considered statistically significant. All experiments were repeated at least three times with similar results.

Results

Heparanase is required for macrophage activation by chemotherapy.

Previous reports have shown that heparanase expression is increased substantially in multiple myeloma patients and cells exposed to chemotherapy (17, 18, 29). Treatment of mesothelioma (MSTO, 2052) and gastric carcinoma (SGC7901) cells with cisplatin, doxorubicin or PCT resulted, nonetheless, in only modest 2-3 fold increase in heparanase expression (Suppl. Fig. 1A). Given the role of heparanase in cells of the tumor microenvironment (24), and more specifically macrophages (22), we examined heparanase expression by J774 macrophages exposed to chemotherapies and found a similar magnitude of heparanase induction (Fig. 1A, upper panel). Unlike heparanase, MIP2 (= CXCL2, GROβ) expression was markedly induced (over 60-fold) in J774 cells exposed to cisplatin or PCT (Fig. 1A, lower panel), suggesting that chemotherapy activates macrophages. In order to ascertain this finding, we exposed primary peritoneal macrophages to PCT and examined the expression of selected cytokines. We found that the expression of TNFα (Fig. 1B, upper panel), MIP2 (Fig.1B, middle panel) and IL10 (Fig. 1B, lower panel) were increased noticeably (15-, 60-, and 10-fold, respectively) in macrophages isolated from C57BL/6 mice exposed to PCT (Fig. 1B, WT). In striking contrast, PCT failed to stimulate cytokine expression in peritoneal macrophages isolated from heparanase-knockout (Hpa-KO) mice (Fig. 1B, KO). However, once Hpa-KO macrophages were supplemented exogenously with recombinant heparanase and then treated with PCT, cytokine induction was re-gained (Fig. 1C). We further examined the induction of MIP2 at the protein level by ELISA. We found that treatment of peritoneal macrophages and J774 cells with PCT and cisplatin (but not doxorubicin) resulted in a marked increase in MIP2 levels (Fig. 2A, middle and lower panels), comparable to MIP2 induction quantified by qPCR (Fig. 2A, upper panel). Moreover, induction of MIP2 and TNFα by PCT was attenuated by the heparanase inhibitor PG545 (Fig. 2B, PG) and even a more prominent inhibition was obtained by the small molecule heparanase inhibitor H1001 (Fig. 2B). The latter compound (Suppl. Fig. 1B) appears unique in its ability to inhibit intracellular (Suppl. Fig. 1C) as well as extracellular (Suppl. Fig. 1D) heparanase, altogether resulting in decreased cell invasion (Suppl. Fig. 1E). In addition, H1001 appears to inhibit heparanase processing (Suppl. Fig. 1F), suggesting that this compound affects heparanase activity at different levels.

PCT-treated macrophages enhance chemoattraction.

To reveal the biological consequences of macrophage activation by chemotherapeutics, we first examined the migration capacity of macrophages in a Boyden chamber apparatus. To this end, WT macrophages were plated in the upper compartment and conditioned medium (CM) collected from control (untreated) and PCT-treated WT and KO macrophages was added as a chemoattractant to the lower compartment. Clearly, medium conditioned by PCT-treated macrophages was far more efficient in eliciting cell migration than medium conditioned by control, untreated, macrophages (Suppl. Fig. 2A, WT; $p<0.01$). Moreover, CM isolated from Hpa-KO macrophages was less efficient in driving macrophage migration (Suppl. Fig. 2A, KO; $p<0.01$). To examine this aspect in an *in vivo* setting, control (untreated) and PCT-treated macrophages were suspended in Matrigel and implanted subcutaneously in WT C57BL/6 mice. Hematoxylin & Eosin staining of Matrigel plugs collected 12 days later showed that plugs containing PCT-treated macrophages attract far more cells (Fig. 2C, upper panel), associating with increased blood vessels density (CD31; Fig. 2C, second panel). Moreover, PCT-treated macrophages induced accumulation of SMA-positive cells, most likely fibroblasts, at the plug periphery (SMA; Fig. 2C, third panels) and far more macrophages evident by immunostaining and real-time PCR (F4/80; Fig. 2C, lower panels, Suppl. Fig. 2B). This suggests that cytokines induced by PCT attract more immune (i.e., macrophages) and non-immune (i.e., fibroblasts) cells to the plug, and promote angiogenesis. Implantation of Matrigel devoid of macrophages failed to attract host cells (Suppl. Fig. 3A).

We next examined the polarization of untreated (control) and PCT/cisplatin-treated macrophages by FACS analyses utilizing cell surface markers typical of M1 ($CD206^{-}$, $CD11c^{+}$) and M2 ($CD206^{+}$, $CD11c^{-}$) macrophages. Untreated WT macrophages were mostly comprised of M1 cells with marginal (less than 1%) polarized M2 cells (Con; Fig. 2D, WT). PCT and cisplatin treatment resulted in a marked, 10-fold increase in the number of M2 macrophages and macrophages that showed both M1 and M2 markers, accompanied by decreased M1 type cells (WT; Fig. 2D, PCT, Cis). In striking contrast, PCT and cisplatin failed to polarize macrophages isolated from Hpa-KO mice (Fig. 2D, KO; Suppl. Fig. 3B), further signifying the role of heparanase in macrophages responses to chemotherapeutic drugs.

PCT-treated macrophages enhance tumor growth.

To elucidate the role of macrophages polarization by PCT in the context of tumor growth, we implanted LLC cells without or with an equal number of untreated (+Con) or PCT-treated (+PCT) macrophages subcutaneously and tumor growth was inspected. This model system was preferred because it was used successfully in a previous study (22). Once implanted in WT C57BL/6 mice, PCT-treated macrophages modestly promoted the growth of LLC tumors (+PCT; Suppl. Fig. 3C), yet this increase in tumor weight was statistically insignificant ($p=0.1$). However, when implanted in Hpa-KO mice, the inclusion of PCT-treated macrophages together with LLC cells resulted in a noticeable increase in tumor weight (Fig. 3A). Thus, while LLC alone or LLC together with control (untreated) macrophages yielded tumors with an average weight of 192 (LLC) and 218 mg (+Con; Fig. 3A), respectively, PCT-treated macrophages resulted in 4-fold increase in tumor weight

(+PCT; 821±79 mg, Fig. 3A), differences that were statistically highly significant (p=0.004 for LLC vs LLC+PCT). This increase in tumor weight was associated with a 7-fold increase in tumor VEGF-A expression levels (Fig. 3B) and tumor vascularity (Fig. 3C). Furthermore, tumors produced by LLC cells and PCT-treated macrophages showed increased MIP2 expression (Fig. 3D, left panel, +PCT), in agreement with our in vitro results (Fig. 1). Also, we found that LLC+PCT tumors show a substantial increase in the expression of Ly6g, a typical marker of neutrophils (+PCT; Fig. 3D, right). Immunostaining of tumor sections revealed that in LLC tumors, neutrophils are mainly detected at the tumor periphery (Fig. 3E, left panels). In contrast, the inclusion of PCT-treated macrophages together with LLC cells resulted in massive recruitment of neutrophils to the tumor periphery and the center of the tumor (Fig. 3E, right panels).

Consistent and robust induction of MIP2 expression by PCT and Cisplatin in vitro and in vivo (Fig. 1B, C; Fig. 2A, B, Fig. 3D), and its critical role in tumorigenesis (30) led us to examine the role of this cytokine in PCT-enhanced tumor growth. To this end, Hpa-KO mice were implanted with LLC+PCT-treated macrophages and were left untreated (+PCT) or were treated with an inhibitor of CXCR2 (SB 225002; +PCT+CXCR2 Inh) (31), the high-affinity receptor of MIP2 (32). Growth of tumors produced by LLC cells inoculated together with PCT-treated macrophages was increased 4 folds vs. tumors produced by LLC alone or LLC+Con macrophages (Fig. 4A), in perfect agreement with the previous experiment (Fig. 3A). Notably, the growth of tumors produced by LLC+PCT-treated macrophages was attenuated markedly by the CXCR2 inhibitor (Fig. 4A, +PCT+CXCR2 Inh). Recruitment of macrophages to tumors produced by LLC+PCT-treated macrophages was increased 6-fold vs. tumors produced by LLC or LLC+Con macrophages (Fig. 4B), and this recruitment, as well as the recruitment of fibroblast activation protein (FAP)/SMA-positive cells, was also reduced by the CXCR2 inhibitor (Fig. 4B, upper panel; Fig. 4C). Moreover, FACS analyses of tumors single-cell suspensions revealed a decrease in M1 macrophages in tumors produced by LLC+PCT-treated macrophages vs. LLC alone or LLC+Con macrophages (Fig. 4B, second panel), accompanied by a parallel increase of M2 macrophages (Fig. 4B, lower panel). Decreased M1 and increased M2 macrophages in tumors produced by LLC+PCT-treated macrophages was reversed by the CXCR2 inhibitor (+PCT+CXCR2 Inh; Fig. 4B, second and lower panels), altogether signifying the critical role of CXCR2 in PCT-mediated macrophages attraction, polarization, and tumor growth.

Activation of macrophages by chemotherapeutics involves heparanase-mediate histone methylation.

In order to reveal the molecular mechanism underlying heparanase-dependent macrophage activation by chemotherapeutics, we examined the methylation status of histones postulated previously to involve heparanase (33). We found that PCT stimulates di- and tri-methylation of lysine 4 of histone 3 (H3K4Me2, Me3) in macrophages isolated from WT mice (WT; Fig. 5A, upper and second panels). In striking contrast, no such increase in H3K4 methylation was noted in macrophages isolated from Hpa-KO mice (KO; Fig. 5A, upper and second panels). Increased H3K4 methylation in WT vs. Hpa-KO macrophages appeared unique because methylation of histone 3 on lysine 27 was induced by PCT to comparable magnitude in macrophages isolated from WT and KO mice (H3K27Me3; Fig. 5A, third

panel). Acetylation of histone H2B on lysine 5 was higher in Hpa-KO macrophages at time 0 and was modestly increased following PCT treatment (Fig. 5A, fourth panels), pointing to H3K4 methylation as the histone alteration most relevant to the differential induction of cytokines in WT vs. KO macrophages (Fig. 1). We further found that Cisplatin elicits a comparable increase in di- and tri-H3K4 methylation in WT but not Hpa-KO macrophages (Fig. 5B) and, moreover, that increased H3K4 methylation by PCT is markedly reduced by the small molecule heparanase inhibitor, H1001 (Fig. 5C). Increased H3K4 methylation by PCT and cisplatin in WT but not KO macrophages was further evident by immunofluorescent staining (Fig. 5D, E). To further tie H3K4 methylation with cytokine expression, we treated cells with an inhibitor of LSD1 (GSK-2879552), an H3K4 demethylase. Indeed, H3K4 methylation was increased substantially (over 7-fold) in WT macrophages treated with GSK-2879552 (Fig. 5F), associating with marked induction of MIP2, IL6, and TNFα (Fig. 5G, 1st, 2nd and 3rd panels, respectively) expression. These results strongly suggest that induced cytokine expression by PCT/cisplatin involves H3K4 methylation.

To reveal the molecular mechanism underlying the increase in heparanase-dependent H3K4 methylation, we first examined the possible involvement of Toll-like receptors (TLR). This was anticipated based on previous reports showing that PCT activates macrophages via TLR (34, 35). We found that the expression of TLR2 and TLR4 is lower in macrophages isolated from Hpa-KO vs. WT mice (Suppl. Fig. 4A, upper and second panels, 0), in agreement with our previous report (22). We also found that TLR2 and TLR4 expression is increased by PCT, but this modest increase was noted in macrophages isolated from WT and KO mice (Suppl. Fig. 4A upper and second panels). Moreover, MIP2 induction by PCT was not affected in macrophages treated with inhibitor of Myd88, an adapter protein used by almost all TLRs (except TLR3) to activate the transcription factor NF-κB (Suppl. Fig. 4A, lower panel), suggesting that the differential response of WT and KO macrophages to PCT in term of cytokine induction is mediated by mechanism(s) other than TLRs. H3K4 methylation is catalyzed by the highly evolutionarily conserved multiprotein complex of methyltransferases known as Set1/COMPASS or MLL/COMPASS-like complexes (36). We, therefore, examined the expression levels of Set1 and MLLs in WT and Hpa-KO macrophages treated with PCT. We found that Set1A and MLL1 expression is profoundly lower in KO vs. WT macrophages, yet their expression was not induced by PCT (Suppl. Fig. 4B, upper and second panels). Moreover, we could not detect a noticeable increase of MLL2, MLL3, MLL4 or RBBP5 in response to PCT nor a differential response of WT vs. KO macrophages (Suppl. Fig. 4B, third-fifth panels; Suppl. Fig. 4C). In striking contrast, the expression of WDR5, an essential component of H3K4 methyltransferase complexes (37), was highly induced by PCT in WT, but not in KO macrophages (Fig. 6A, left). WDR5 expression was highly induced, nonetheless, in KO macrophages supplemented exogenously with heparanase and then treated with PCT (Fig. 6A, middle and right panels), closely resembling the induction of cytokines in this experimental setting (Fig. 1C). We further confirmed WDR5 induction in WT but not Hpa-KO macrophages by immunoblotting (Fig. 6B). WDR5 induction by WT macrophages was also evidenced by immunofluorescent staining (Fig. 6C). Notably, induction of MIP2, TNFα, and IL6 by PCT was reduced prominently in cells treated with WDR5 inhibitor (OICR-9429; Fig. 6D; Suppl. Fig. 5A). These results point to

WDR5 as the molecular determinant that mediates macrophage activation by PCT and reveal WDR5 as a novel gene under heparanase regulation.

Discussion

Evidence accumulating in the last two decades have critically staged heparanase at the heart of tumor progression and metastasis (6-8). This led basic researchers and biotechnology companies to develop heparanase inhibitors, some of which (i.e., PG545= Pixatimod) are being evaluated in advanced clinical trials alone, and in combination with other drugs (38). Less attention was, nonetheless, directed toward deciphering the role of heparanase in cells that constitute the tumor microenvironment and thought to play an instrumental role in tumorigenesis (39, 40).

We and others have reported previously that heparanase is expressed by macrophages and is intimately involved in cytokine gene regulation (22, 25, 41). Here, we show that activation and polarization of macrophages by chemotherapy is also heparanase-dependent, thus extending the repertoire of heparanase function in macrophages.

In agreement with earlier reports (42), we found that macrophages are stimulated by PCT and cisplatin to express much higher levels of cytokines. Notably, and unlike WT macrophages, peritoneal macrophages isolated from Hpa-KO mice failed to increase cytokine expression following PCT and cisplatin treatment (Fig. 1B); these macrophages, nevertheless, retained the capacity to respond to PCT once heparanase is provided (Fig. 1C), or upon treatment with medium conditioned by WT macrophages exposed to PCT (Suppl. Fig. 5B). Moreover, cytokines induction by PCT was attenuated substantially by the heparanase inhibitor PG545 (HS mimetic) (43) and even more so by the small-molecule heparanase inhibitor H1001 (Fig. 2B). This compound appears unique in its ability to inhibit endogenous heparanase. This emerged from reduced heparanase activity in cell extracts following addition of H1001 to the cell culture medium (Suppl. Fig. 1C), thus possibly inhibiting heparanase functions that take place inside the cell (44). Even more dramatic was the ability of chemotherapy to polarize WT, but not Hpa-KO macrophages towards M2-like phenotype (Fig. 2D), clearly indicating that heparanase is critical for macrophages polarization by chemotherapy. Consequently, PCT-treated WT macrophages promoted the growth of LLC tumors. This trend was evident in WT mice (Suppl. Fig. 3C) and became highly significant in Hpa-KO mice (Figs. 3A, 4A), associating with a marked increase in VEGF-A expression and tumor vascularity (Fig. 3B, C). The reason for the more extreme phenotype in the growth of tumors implanted in Hpa-KO vs. WT mice is not entirely clear, but likely involves the inability of KO macrophages to populate the tumor. We have shown previously that LLC cells develop smaller tumors in Hpa-KO vs. WT mice (22). Decreased tumor growth was associated with a lower number of macrophages being recruited to the tumors and, moreover, their localization. Thus, while macrophages populated the entire tumor mass in WT mice, they were arrested at the periphery of tumors developed in Hpa-KO mice (22), implying that heparanase is required for macrophages penetration into the tumors. This may suggest that host macrophages attracted to the tumor compromise the effect of PCT-treated macrophages implanted together with LLC cells. In Hpa-KO mice, on the other hand, host macrophages do not populate the tumors, and the effect of PCT on the implanted

macrophages is not compromised. Unlike macrophages, neutrophils seem not to be dependent on heparanase for their migration into inflamed tissues (45) and massively populate the tumors produced by co-injection of LLC cells and PCT-treated macrophages (Fig. 3E, right panels), likely promoting tumor growth (46). Increased recruitment of neutrophils was also confirmed by qPCR for Ly6g (Fig. 3D, right) and was associated with a comparable increase of MIP2 (Fig. 3D, left) that functions as a chemoattractant for neutrophils and macrophages (47). Indeed, blocking CXCR2 blunted tumor growth evoked by PCT (Fig. 4A), and prevented the recruitment and polarization of macrophages toward M2 while increasing the M1 type (Fig. 4B). This points to CXCR2 as an important player in the adverse effects of chemotherapy and justifies its targeting along with PCT (48). It should be noted that CXCR2 functions as a receptor to cytokines other than MIP2 so that the observed phenotypes cannot be attributed solely to MIP2. However, we did not find changes in the expression of CXCL1 or CXCL5 (Suppl. Fig. 5C, D) in this experimental setting and their relevance to these results is questionable.

The molecular mechanism underlying the activation of WT, but not Hpa-KO, macrophages by PCT/cisplatin appears to involve histone methylation. Clearly, di- and tri-methylation of H3K4 were prominently increased in WT macrophages by PCT and cisplatin (Fig. 5A, B, D; WT). In striking contrast, no such increase was found in PCT/cisplatin-treated Hpa-KO macrophages (Fig. 5A, B, E; KO). Likewise, H3K4 methylation by PCT was attenuated markedly by the heparanase inhibitor H1001 (Fig. 5C), correlating with decreased MIP2 and TNFα expression (Fig. 2B). Moreover, inhibition of LSD1 that functions as H3K4 demethylase (49, 50), resulted in increased H3K4 methylation, as expected, and most importantly increased cytokine expression (Fig. 5F, G). This result evidently links H3K4 methylation and cytokine expression, in agreement with the notion that H3K4 methylation marks active transcription (49). Importantly, meta-analysis revealed that cancer patients exhibiting a lower level of H3K4 tri-methylation are expected to have longer overall survival (51). This, and the finding that increased H3K4 methylation by PCT/cisplatin is heparanase-dependent (Fig. 5A-E), may provide another explanation for the shorter overall survival of cancer patients exhibiting high levels of heparanase (6-9), yet this possibility awaits further confirmation and clinical validation. Finally, we discovered that cytokine induction by PCT involves WDR5. Unlike other components of the COMPASS complex (i.e., SET1A, MLL1-4, RBBP5, Ash2L, LEDGF; Suppl. Fig. 4B, Suppl. Fig. 4C, Suppl. Fig. 5E), expression of WDR5 was induced over 10-fold by PCT in WT but not Hpa-KO macrophages. Furthermore, increased WDR5 expression was evident already 2 hours after PCT addition and persisted for further 24 hours (Fig. 6A, B), likely leading to cytokine induction at later time points (Fig. 1B). Moreover, the expression of megakaryocytic leukemia 1 (MKL1) that potentiates the binding of WDR5 to specific promoter region of target genes (37) exhibited a similar expression pattern (Suppl. Fig. 6A), further supporting the role of WDR5 in cytokine induction by PCT. Most importantly, inhibition of WDR5 or MKL1 practically prevents the induction of cytokines by PCT (Fig. 6D, Suppl. Fig. 5A; Suppl. Fig. 6B), thus supporting the critical role of WDR5 in macrophages induction by chemotherapy. In addition, overexpression of WDR5 enhanced, whereas WDR5 gene silencing reduced MIP2 expression (Suppl. Fig. 6C, D), thus critically linking the COMPASS complex with cytokine gene expression. The observation that SET1A, MLL1,

and MKL1 expression is significantly lower in KO macrophages (Suppl. Fig. 4B, Suppl. Fig. 6A) strongly implies that the COMPASS complex is impaired in the absence of heparanase, resulting in decreased H3K4 methylation (Fig. 5A, B; Fig. 7).

The mode by which heparanase regulates the expression of COMPASS genes is not entirely clear but may involve the interaction of heparanase with the promoter and transcribed regions of transcriptionally active genes as was found in Jurkat T cells (33). Alternatively, gene regulation by heparanase may result from cleavage of nuclear HS, altering the chromatin structure (52), or signal transduction potentiated by heparanase. For example, phosphorylation of JNK was increased markedly in WT macrophages treated with PCT. In striking contrast, only minimal increase in JNK phosphorylation was elicited in KO macrophages (Suppl. Fig. 7A, upper panels; Suppl. Fig. 7B). Importantly, increased H3K4 methylation and cytokine induction by PCT was prevented by JNK and p38 inhibitors (Suppl. Fig. 7C, D), thus connecting PCT, stress signals (JNK, p38), histone methylation and cytokine expression. Noteworthy, the expression of BiP, indicative of ER stress, was higher in Hpa-KO vs WT macrophages (Suppl. Fig. 7A, right lower panel), suggesting that PCT effect is specific for the stress arm of the MAPK pathway.

Taken together, we show for the first time that activation of macrophages by chemotherapy is heparanase-dependent. We further delineate the molecular mechanism underlying this novel function of heparanase to involve WDR5 induction and H3K4 methylation. This is highly significant given the key roles of WDR5 in the progression of a variety of cancers involving transcriptional activation of oncogenes, EMT-related genes, and genes involved in lymph-angiogenesis and tumor metastasis, among other pro-tumorigenic properties (37, 53, 54). This unique mechanism provides a new perspective for the unfortunate pro-cancer function of chemotherapy (12, 55), yet offers new treatment modalities (i.e., WDR5 inhibitors, H1001) to optimize chemotherapeutics. This approach deems promising, but it should be kept in mind that heparanase plays a role also in the recruitment of cells with anti-tumor activity such as NK cells (56). Thus, heparanase inhibitors should be applied in a personalized manner, where NK cells are less abundant.

Supplementary Material

Refer to Web version on PubMed Central for supplementary material.

Acknowledgments

We are grateful to Dr. Nili Schutz (HepaRx Ltd., Ness-Ziona, Israel) for kindly providing the heparanase inhibitor H1001. This study was generously supported by research grants awarded to RS and IV by the National Institutes of Health (CA211752) and the United States-Israel Binational Science Foundation (BSF). It was also supported by grants from the Israel Science Foundation (grant 601/14), the ISF-NSFC joint research program (grant No. 2572/16 awarded to I.V and S-M.Y), and the Israel Cancer Research Fund (ICRF) awarded to I.V., and by an ERC grant (number 771112) awarded to YS. UB was supported by a postdoctoral fellowship awarded by the Israeli Council for higher education. I. Vlodavsky is a Research Professor of the ICRF.

References

1. Freeman C, Browne AM, Parish CR. Evidence that platelet and tumour heparanases are similar enzymes. Biochem J. 1999;342 (Pt 2):361–8. [PubMed: 10455023]

2. Vlodavsky I, Friedmann Y. Molecular properties and involvement of heparanase in cancer metastasis and angiogenesis. J Clin Invest. 2001;108:341–7. [PubMed: 11489924]
3. Bame KJ. Heparanases: endoglycosidases that degrade heparan sulfate proteoglycans. Glycobiology. 2001;11:91R–8R.
4. Parish CR, Freeman C, Hulett MD. Heparanase: a key enzyme involved in cell invasion. Biochim Biophys Acta. 2001;1471:M99–108. [PubMed: 11250066]
5. Parish CR. The role of heparan sulphate in inflammation. Nat Rev Immunol. 2006;6:633–43. [PubMed: 16917509]
6. Vlodavsky I, Singh P, Boyango I, Gutter-Kapon L, Elkin M, Sanderson RD, et al. Heparanase: From basic research to therapeutic applications in cancer and inflammation. Drug Resist Updates. 2016;29:54–75.
7. Rivara S, Milazzo FM, Giannini G. Heparanase: a rainbow pharmacological target associated to multiple pathologies including rare diseases. Future Med Chem. 2016;8:647–80. [PubMed: 27057774]
8. Vlodavsky I, Gross-Cohen M, Weissmann M, Ilan N, Sanderson RD. Opposing functions of heparanase-1 and heparanase-2 in cancer progression. Trends Biochem Sci. 2018;43:18–31. [PubMed: 29162390]
9. Vreys V, David G. Mammalian heparanase: what is the message? J Cell Mol Med. 2007;11:427–52. [PubMed: 17635638]
10. Hammond E, Khurana A, Shridhar V, Dredge K. The role of heparanase and sulfatases in the modification of heparan sulfate proteoglycans within the tumor microenvironment and opportunities for novel cancer therapeutics. Front Oncol. 2014;4:195. [PubMed: 25105093]
11. Vlodavsky I, Ilan N, Naggi A, Casu B. Heparanase: structure, biological functions, and inhibition by heparin-derived mimetics of heparan sulfate. Curr Pharm Des. 2007;13:2057–73. [PubMed: 17627539]
12. Shaked Y Balancing efficacy of and host immune responses to cancer therapy: the yin and yang effects. Nat Rev Clin Oncol. 2016;13:611–26. [PubMed: 27118493]
13. Gingis-Velitski S, Loven D, Benayoun L, Munster M, Bril R, Voloshin T, et al. Host response to short-term, single-agent chemotherapy induces matrix metalloproteinase-9 expression and accelerates metastasis in mice. Cancer Res. 2011;71:6986–96. [PubMed: 21978934]
14. Daenen LG, Roodhart JM, van Amersfoort M, Dehnad M, Roessingh W, Ulfman LH, et al. Chemotherapy enhances metastasis formation via VEGFR-1-expressing endothelial cells. Cancer Res. 2011;71:6976–85. [PubMed: 21975929]
15. Yamauchi K, Yang M, Hayashi K, Jiang P, Yamamoto N, Tsuchiya H, et al. Induction of cancer metastasis by cyclophosphamide pretreatment of host mice: an opposite effect of chemotherapy. Cancer Res. 2008;68:516–20. [PubMed: 18199547]
16. Middleton JD, Stover DG, Hai T. Chemotherapy-Exacerbated Breast Cancer Metastasis: A Paradox Explainable by Dysregulated Adaptive-Response. Int J Mol Sci. 2018;19.
17. Ramani VC, Vlodavsky I, Ng M, Zhang Y, Barbieri P, Noseda A, et al. Chemotherapy induces expression and release of heparanase leading to changes associated with an aggressive tumor phenotype. Matrix Biol. 2016;55:22–34. [PubMed: 27016342]
18. Ramani VC, Zhan F, He J, Barbieri P, Noseda A, Tricot G, et al. Targeting heparanase overcomes chemoresistance and diminishes relapse in myeloma. Oncotarget. 2016;7:1598–607. [PubMed: 26624982]
19. Barash U, Lapidot M, Zohar Y, Loomis C, Moreira A, Feld S, et al. Involvement of heparanase in the pathogenesis of mesothelioma: Basic aspects and clinical applications. J Natl Cancer Inst. 2018;110:1102–14. [PubMed: 29579286]
20. Barash U, Spyrou A, Liu P, Vlodavsky E, Zhu C, Luo J, et al. Heparanase promotes glioma progression via enhancing CD24 expression. Intl J Cancer. 2019;145:1596–608.
21. Tang B, Xie R, Qin Y, Xiao YF, Yong X, Zheng L, et al. Human telomerase reverse transcriptase (hTERT) promotes gastric cancer invasion through cooperating with c-Myc to upregulate heparanase expression. Oncotarget. 2016;7:11364–7. [PubMed: 26689987]

22. Gutter-Kapon L, Alishekevitz D, Shaked Y, Li JP, Aronheim A, Ilan N, et al. Heparanase is required for activation and function of macrophages. Proc Natl Acd Sci USA. 2016;113:E7808–E17.

23. Vlodavsky I Preparation of extracellular matrices produced by cultured corneal endothelial and PF-HR9 endodermal cells In: Bonifacino JS MD, Hartford JB, Lippincott-Schwartz J and Yamada KM., editor. Protocols in Cell Biology. New York: John Wiley & Sons; 1999 p. 10.4.1–.4.4.

24. Weissmann M, Arvatz G, Horowitz N, Feld S, Naroditsky I, Zhang Y, et al. Heparanase-neutralizing antibodies attenuate lymphoma tumor growth and metastasis. Proc Natl Acad Sci USA. 2016;113:704–9. [PubMed: 26729870]

25. Blich M, Golan A, Arvatz G, Sebbag A, Shafat I, Sabo E, et al. Macrophage activation by heparanase is mediated by TLR-2 and TLR-4 and associates with plaque progression. Arterioscl, Throm, Vas Biol. 2013;33:e56–65.

26. Gingis-Velitski S, Zetser A, Flugelman MY, Vlodavsky I, Ilan N. Heparanase induces endothelial cell migration via protein kinase B/Akt activation. J Biol Chem. 2004;279:23536–41. [PubMed: 15044433]

27. Shteingauz A, Ilan N, Vlodavsky I. Processing of heparanase is mediated by syndecan-1 cytoplasmic domain and involves syntenin and alpha-actinin. Cell Mol Life Sci. 2014;71:4457–70. [PubMed: 24788042]

28. Voloshin T, Alishekevitz D, Kaneti L, Miller V, Isakov E, Kaplanov I, et al. Blocking IL1beta pathway following paclitaxel chemotherapy slightly inhibits primary tumor growth but promotes spontaneous metastasis. Mol Cancer Ther. 2015;14:1385–94. [PubMed: 25887886]

29. Bandari SK, Purushothaman A, Ramani VC, Brinkley GJ, Chandrashekar DS, Varambally S, et al. Chemotherapy induces secretion of exosomes loaded with heparanase that degrades extracellular matrix and impacts tumor and host cell behavior. Matrix Bio. 2018;65:104–18. [PubMed: 28888912]

30. Burger M, Burger JA, Hoch RC, Oades Z, Takamori H, Schraufstatter IU. Point mutation causing constitutive signaling of CXCR2 leads to transforming activity similar to Kaposi's sarcoma herpesvirus-G protein-coupled receptor. J Immunol. 1999;163:2017–22. [PubMed: 10438939]

31. Bento AF, Leite DF, Claudino RF, Hara DB, Leal PC, Calixto JB. The selective nonpeptide CXCR2 antagonist SB225002 ameliorates acute experimental colitis in mice. J Leukocyte Biol. 2008;84:1213–21. [PubMed: 18653784]

32. Rosenkilde MM, Schwartz TW. The chemokine system -- a major regulator of angiogenesis in health and disease. Apmis. 2004;112:481–95. [PubMed: 15563311]

33. He YQ, Sutcliffe EL, Bunting KL, Li J, Goodall KJ, Poon IK, et al. The endoglycosidase heparanase enters the nucleus of T lymphocytes and modulates H3 methylation at actively transcribed genes via the interplay with key chromatin modifying enzymes. Transcription. 2012;3:130–45. [PubMed: 22771948]

34. Ding AH, Porteu F, Sanchez E, Nathan CF. Shared actions of endotoxin and taxol on TNF receptors and TNF release. Science. 1990;248:370–2. [PubMed: 1970196]

35. Kawasaki K, Akashi S, Shimazu R, Yoshida T, Miyake K, Nishijima M. Mouse toll-like receptor 4.MD-2 complex mediates lipopolysaccharide-mimetic signal transduction by Taxol. J Biol Chem. 2000;275:2251–4. [PubMed: 10644670]

36. Qu Q, Takahashi YH, Yang Y, Hu H, Zhang Y, Brunzelle JS, et al. Structure and conformational dynamics of a COMPASS histone H3K4 methyltransferase complex. Cell. 2018;174:1117–26 e12. [PubMed: 30100186]

37. Trievel RC, Shilatifard A. WDR5, a complexed protein. Nat Struct Mol Biol. 2009;16:678–80. [PubMed: 19578375]

38. Dredge K, Brennan TV, Hammond E, Lickliter JD, Lin L, Bampton D, et al. A Phase I study of the novel immunomodulatory agent PG545 (pixatimod) in subjects with advanced solid tumours. Br J Cancer. 2018;118:1035–41. [PubMed: 29531325]

39. Blonska M, Agarwal NK, Vega F. Shaping of the tumor microenvironment: Stromal cells and vessels. Semin Cancer Biol. 2015.

40. Werb Z, Lu P. The Role of Stroma in Tumor Development. Cancer J. 2015;21:250–3. [PubMed: 26222075]

41. Goodall KJ, Poon IK, Phipps S, Hulett MD. Soluble heparan sulfate fragments generated by heparanase trigger the release of pro-inflammatory cytokines through TLR-4. PloS one. 2014;9:e109596. [PubMed: 25295599]
42. Bogdan C, Ding A. Taxol, a microtubule-stabilizing antineoplastic agent, induces expression of tumor necrosis factor alpha and interleukin-1 in macrophages. J Leukocyte Biol. 1992;52:119–21. [PubMed: 1353517]
43. Dredge K, Hammond E, Handley P, Gonda TJ, Smith MT, Vincent C, et al. PG545, a dual heparanase and angiogenesis inhibitor, induces potent anti-tumour and anti-metastatic efficacy in preclinical models. Br J Cancer. 2011;104:635–42. [PubMed: 21285983]
44. Shteingauz A, Boyango I, Naroditsky I, Hammond E, Gruber M, Doweck I, et al. Heparanase enhances tumor growth and chemoresistance by promoting autophagy. Cancer Res. 2015;75:3946–57. [PubMed: 26249176]
45. Stoler-Barak L, Petrovich E, Aychek T, Gurevich I, Tal O, Hatzav M, et al. Heparanase of murine effector lymphocytes and neutrophils is not required for their diapedesis into sites of inflammation. FASEB J. 2015;29:2010–21. [PubMed: 25634957]
46. Hurt B, Schulick R, Edil B, El Kasmi KC, Barnett C Jr. Cancer-promoting mechanisms of tumor-associated neutrophils. Am J Surg. 2017;214:938–44. [PubMed: 28830617]
47. Charo IF, Ransohoff RM. The many roles of chemokines and chemokine receptors in inflammation. New Engl J Med. 2006;354:610–21. [PubMed: 16467548]
48. Ijichi H, Chytil A, Gorska AE, Aakre ME, Bierie B, Tada M, et al. Inhibiting Cxcr2 disrupts tumor-stromal interactions and improves survival in a mouse model of pancreatic ductal adenocarcinoma. J Clin Invest. 2011;121:4106–17. [PubMed: 21926469]
49. Hyun K, Jeon J, Park K, Kim J. Writing, erasing and reading histone lysine methylations. Exp Mol Med. 2017;49:e324. [PubMed: 28450737]
50. Schapira M Chemical Inhibition of Protein Methyltransferases. Cell Chem Biol. 2016;23:1067–76. [PubMed: 27569753]
51. Li S, Shen L, Chen KN. Association between H3K4 methylation and cancer prognosis: A meta-analysis. Thorac Cancer. 2018;9:794–9. [PubMed: 29737623]
52. Schubert SY, Ilan N, Shushy M, Ben-Izhak O, Vlodavsky I, Goldshmidt O. Human heparanase nuclear localization and enzymatic activity. Lab Invest. 2004;84:535–44. [PubMed: 15034597]
53. Grebien F, Vedadi M, Getlik M, Giambruno R, Grover A, Avellino R, et al. Pharmacological targeting of the Wdr5-MLL interaction in C/EBPalpha N-terminal leukemia. Nat Chem Biol. 2015;11:571–8. [PubMed: 26167872]
54. Lu K, Tao H, Si X, Chen Q. The histone H3 lysine 4 presenter WDR5 as an oncogenic protein and novel epigenetic target in cancer. Front Oncol. 2018;8:502. [PubMed: 30488017]
55. Ebos JM. Prodding the Beast: Assessing the Impact of Treatment-Induced Metastasis. Cancer Res. 2015;75:3427–35. [PubMed: 26229121]
56. Mayfosh AJ, Baschuk N, Hulett MD. Leukocyte Heparanase: A Double-Edged Sword in Tumor Progression. Front Oncol. 2019;9:331. [PubMed: 31110966]

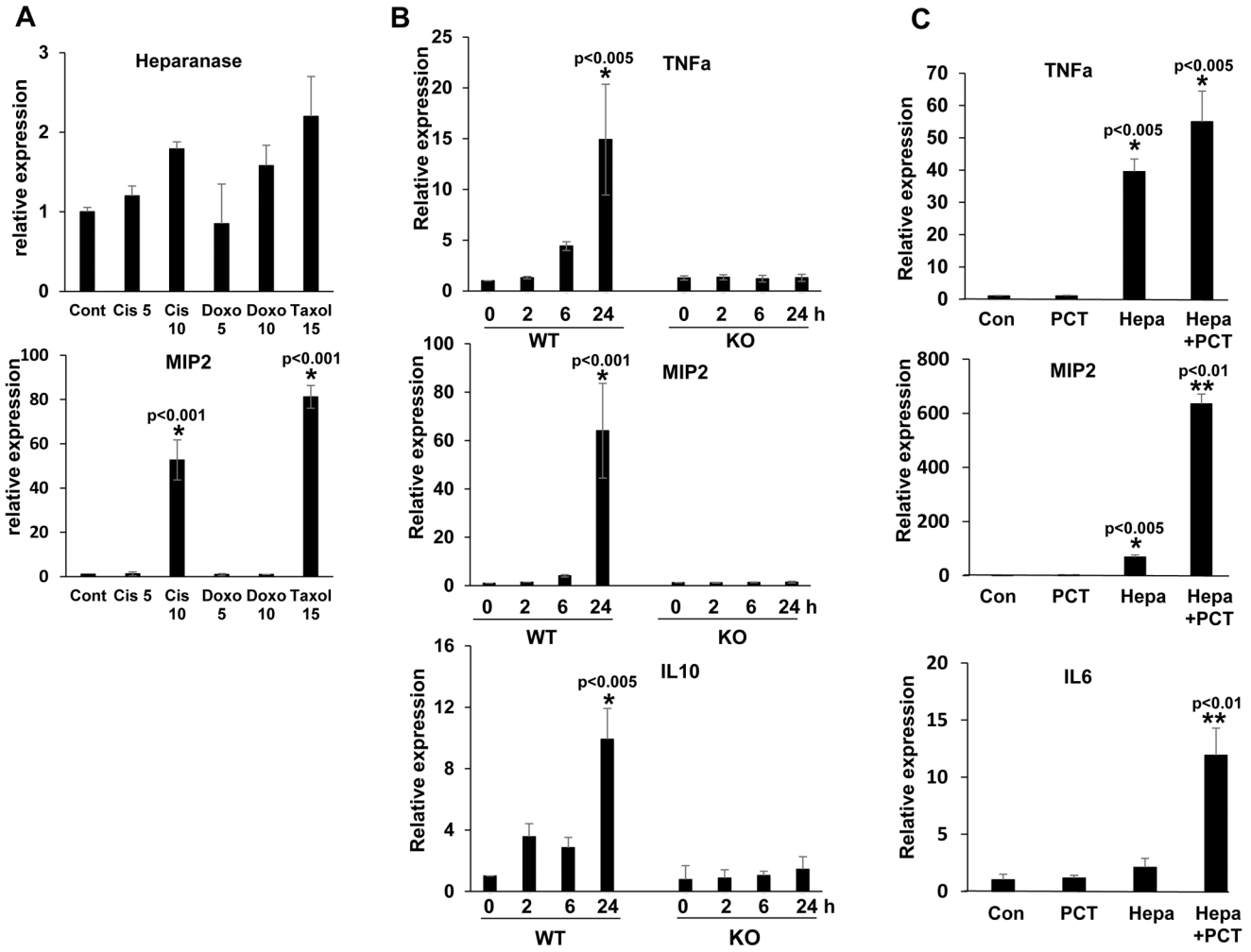

Figure 1.

PCT stimulates cytokine expression in WT but not Hpa-KO macrophages. **A**. Heparanase expression. J774 cells were left untreated (Cont) or were treated with the indicated concentrations of cisplatin (Cis), doxorubicin (Doxo), or PCT for 24 h. Total RNA was then extracted and subjected to qPCR analysis applying primer set specific for mouse heparanase (upper panel). *****p<0.001 vs. Cont. **B**. Cytokine induction by PCT is heparanase-dependent. Peritoneal macrophages were isolated from wild type (WT) and Hpa-KO mice and were treated with PCT (15 μg/ml); Total RNA was extracted at the time indicated and subjected to qPCR applying primers sets specific for TNFα (upper panel), MIP2 (second panel), and IL10 (lower panel). Induction of MIP2 by chemotherapy was also observed in J774 cells (**A**, second panel). *****p<0.005 vs time 0 (control). **C**. Heparanase reconstitution. Macrophages were isolated from Hpa-KO mice and were left untreated (Con), or were added with PCT, heparanase (Hepa; 1 μg/ml), or both. After 24 h total RNA was extracted and subjected to qPCR applying primers specific for TNFα (upper panel), MIP2 (second panel), and IL6 (lower panel). *****p<0.005 vs Con; ******p<0.01 Hepa+PCT vs. Hepa.

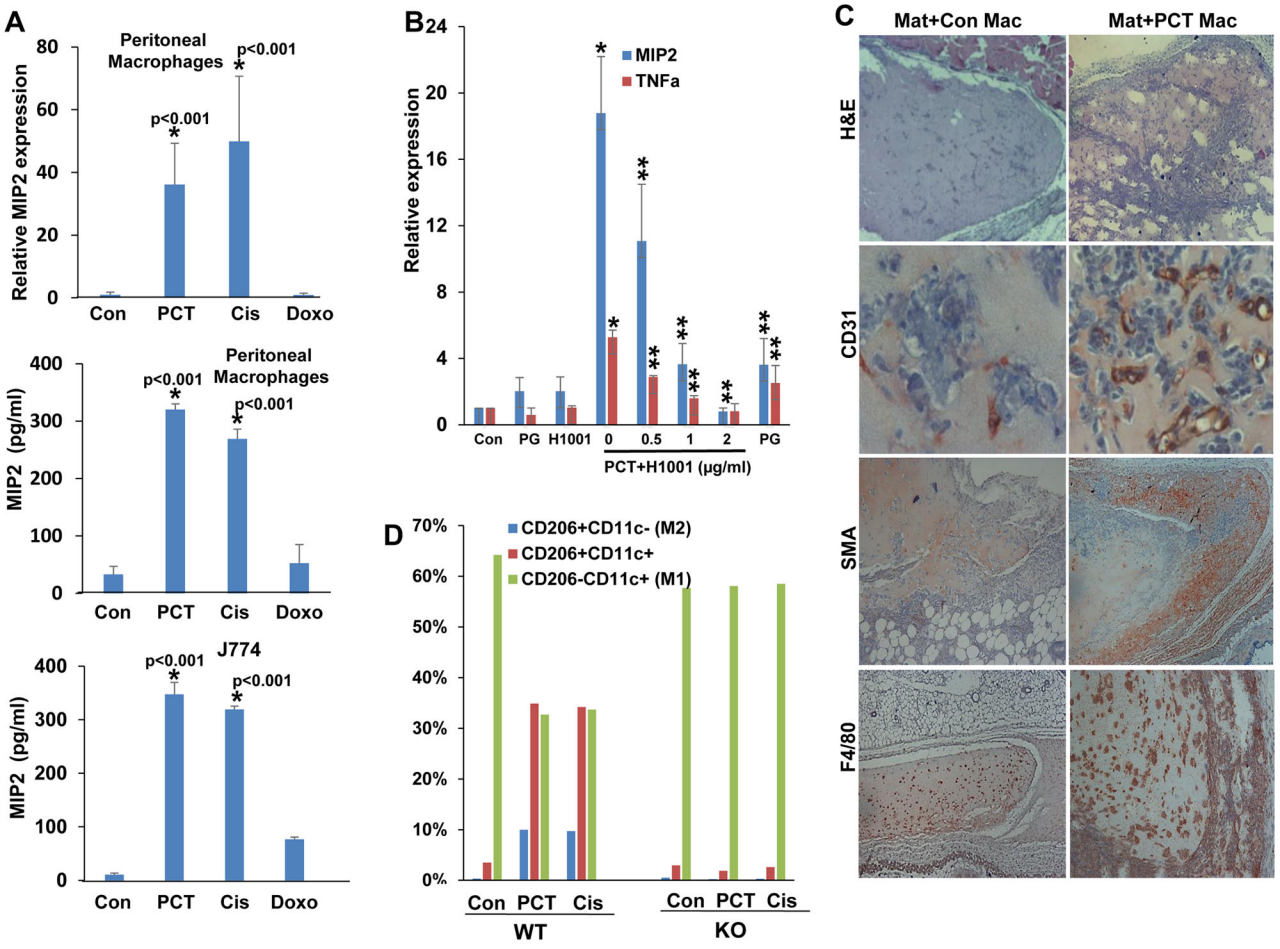

Figure 2.

Chemotherapy stimulates cytokine expression, Matrigel plugs cellularity, and polarization of WT but not Hpa-KO macrophages. **A**. MIP2 induction. Macrophages were isolated from WT mice and were left untreated (Con) or were treated with PCT (15 μg/ml), cisplatin (Cis, 10 μg/ml) or doxorubicin (Doxo, 10 μg/ml) for 24 h. Total RNA was then extracted and subjected to qPCR analysis applying MIP2 specific primers (upper panel). Conditioned medium was collected from corresponding cell cultures, and MIP2 levels were quantified by ELISA (second panel). MIP2 levels were similarly quantified in control (untreated) and chemotherapy-treated J774 cells (lower panel). *p<0.001 PCT/Cis vs. Con. **B**. Peritoneal macrophages were isolated from WT mice and were treated with PCT without (0) or with the indicated concentration of the heparanase inhibitors H1001 or PG545. H1001 (2 μg/ml) and PG545 (50 μg/ml) were also added to macrophages without PCT. After 24 h, total RNA was extracted and subjected to qPCR analyses applying primers specific for MIP2 (blue bars) and TNFα (red bars). Note that cytokine induction by PCT is attenuated markedly by the heparanase inhibitors. *p<0.001 PCT vs. Con; **p<0.01 PCT+H1001 vs. PCT. **C**. Matrigel plugs. WT peritoneal macrophages were left untreated (Con) or were treated with PCT for 24 h. Macrophages were then detached, suspended in Matrigel (Mat) (3×10^6/ml) and implanted (0.5 ml/mouse) in WT C57BL/6 mice. After 12 days plugs were excised, formalin-fixed, paraffin-embedded, and 5-micron sections were subjected to immunostaining

applying anti-CD31 (second panels), anti-SMA (third panels), and anti-F4/80 (lower panels) antibodies. Hematoxylin & Eosin staining is shown in the upper panels. Note increased cellularity, vascularity, and recruitment of host cells to Matrigel plugs embedded with PCT-treated macrophages (Mat+PCT Mac). Original magnifications: upper, third and fourth panels x 25; second panels: x100. **D**. Macrophages polarization. Peritoneal macrophages were isolated from WT and Hpa-KO mice and were left untreated (Con) or were treated with PCT (15 μg/ml) or cisplatin (Cis; 10 μg/ml). After 24 h, cells were detached and subjected to FACS analyses with anti-CD206 and anti-CD11c antibodies. Note that PCT and cisplatin affect the polarization of WT but not Hpa-KO macrophages.

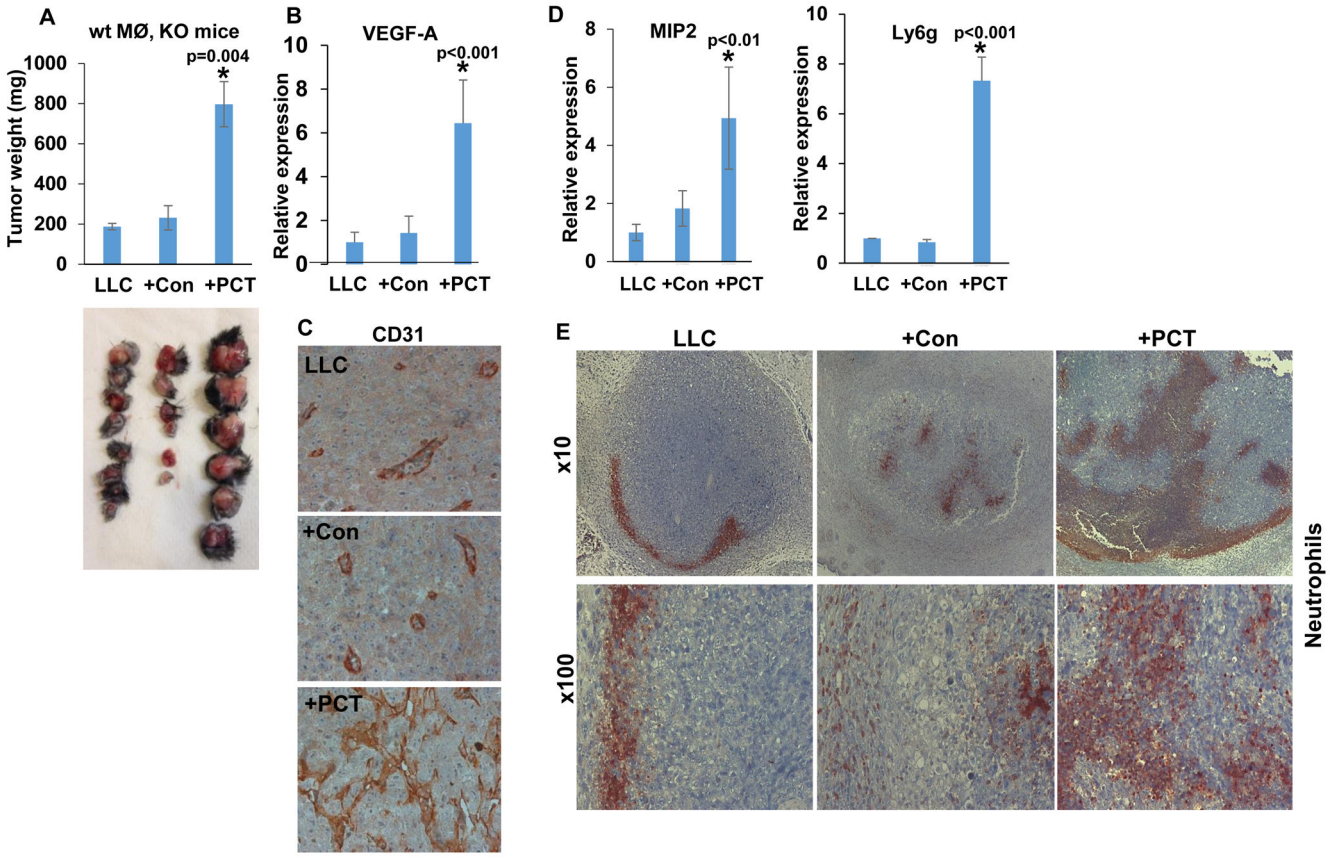

Figure 3.

PCT-treated macrophages promote tumor growth and vascularity. **A**. Tumor growth. LLC cells (4×10^5) were inoculated subcutaneously in Hpa-KO female mice (8-10 weeks old) without (LLC; n=8) or with an equal number of untreated (+Con; n=6) or PCT-treated (+PCT; n=6) macrophages. At termination on day 21, tumors were excised, weighed (upper panel) and photographed (lower panel). *p=0.004 +PCT vs LLC/+Con. Total RNA was extracted from a portion of the tumors and subjected to qPCR applying VEGF-A specific primers (**B**; p<0.01 +PCT vs. LLC/+Con). The rest of the tumors were fixed in formalin, embedded in paraffin and five-micron sections were subjected to immunostaining applying anti-CD31 antibody (**C**). Note increased vascularity of LLC tumors inoculated with PCT-treated macrophages. Original magnifications: x100. Tumor samples were similarly subjected to qPCR applying primers specific for MIP2 (**D**, left) and Ly6g (a marker for neutrophils; **D**, right). p<0.01 +PCT vs. LLC). **E**. Tumor sections were subjected to immunostaining applying anti-Ly6g antibody. Note the recruitment of neutrophils to LLC tumors implanted together with PCT-treated macrophages. Original magnifications: upper panels x10, lower panels: x100.

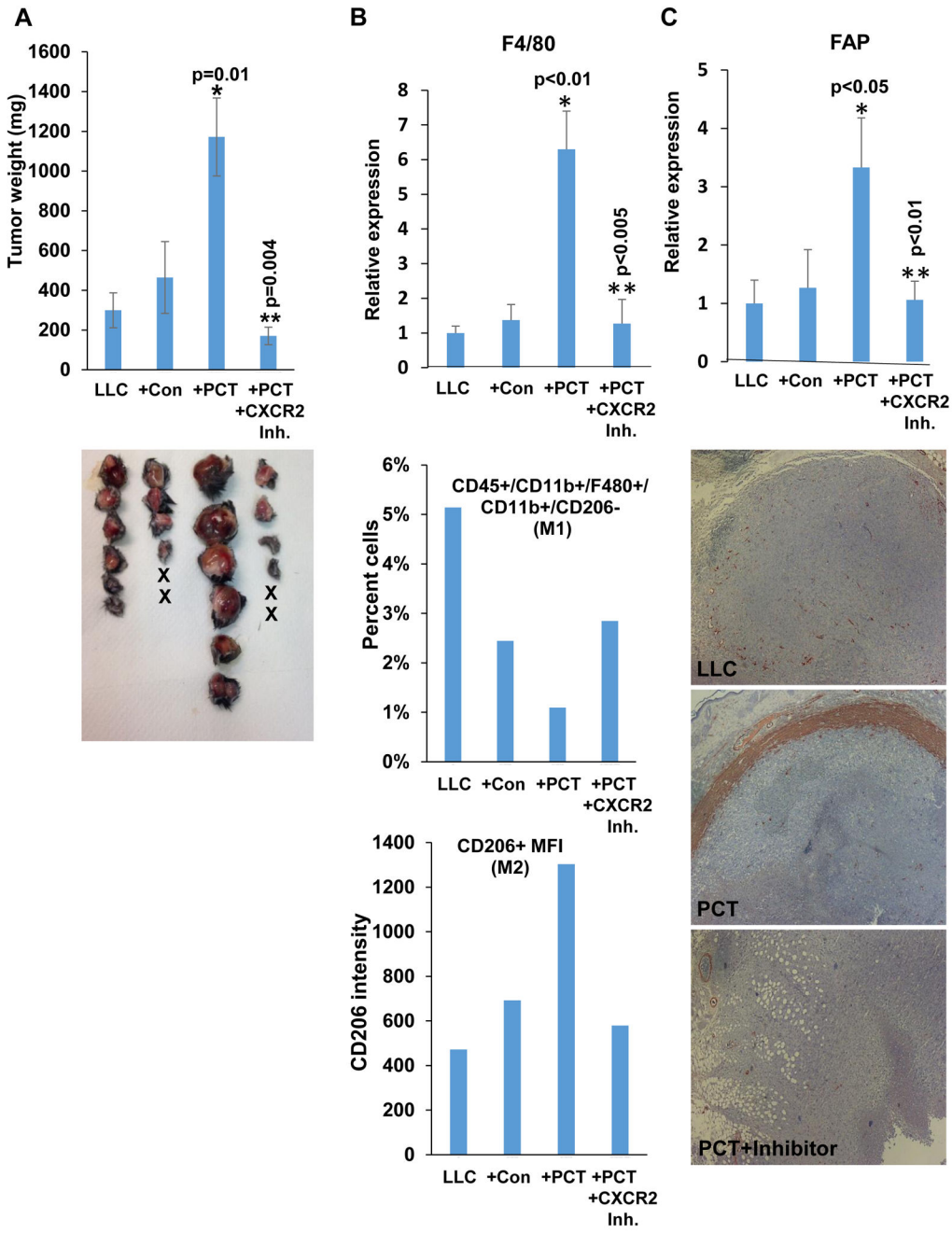

Figure 4.

Enhanced tumor growth by PCT-treated macrophages is mediated by CXCR2. **A**. Tumor growth. LLC cells (4×10^5) were inoculated subcutaneously in Hpa-KO mice without (LLC; n=6) or with an equal number of untreated (+Con; n=6) or PCT-treated (+PCT; n=6) macrophages. Mice inoculated with LLC and PCT-treated macrophages were treated with SB225002 (1.5 mg/kg, i.p once daily in DMSO), an inhibitor of CXCR2, or control vehicle (DMSO). At termination on day 23, tumors were excised, weighed (upper panel) and photographed (lower panel). *p=0.01 +PCT vs +Con; **p=0.004 +PCT vs +PCT+CXCR2 inhibitor. Total RNA was extracted from a portion of the tumors and subjected to qPCR

applying F4/80 specific primers (**B**, upper panel). *p<0.01+PCT vs. LLC;**p<0.005 +PCT +CXCR2 Inh vs +PCT. Single-cell suspensions of the tumors were subjected to FACS analyses. The ratio of M1-macrophages (i.e., $CD45^{+}CD11b^{+}F4/80^{+}CD206^{-}CD11c^{+}$) is shown graphically as a percent of the total cell number (**B**, second panel). Quantification of median fluorescence intensity (MFI) of CD206 (M2 macrophages) is shown in **B**, lower panel. The rest of the tumors were fixed in formalin, embedded in paraffin and five-micron sections were subjected to immunostaining applying anti-SMA antibody (**C**, lower panels). Original magnifications: x25. qPCR of fibroblast activation protein (FAP) alpha is shown in **C**, upper panel. *p<0.05 +PCT vs. LLC;**p<0.01 +PCT+CXCR2 Inh vs +PCT.

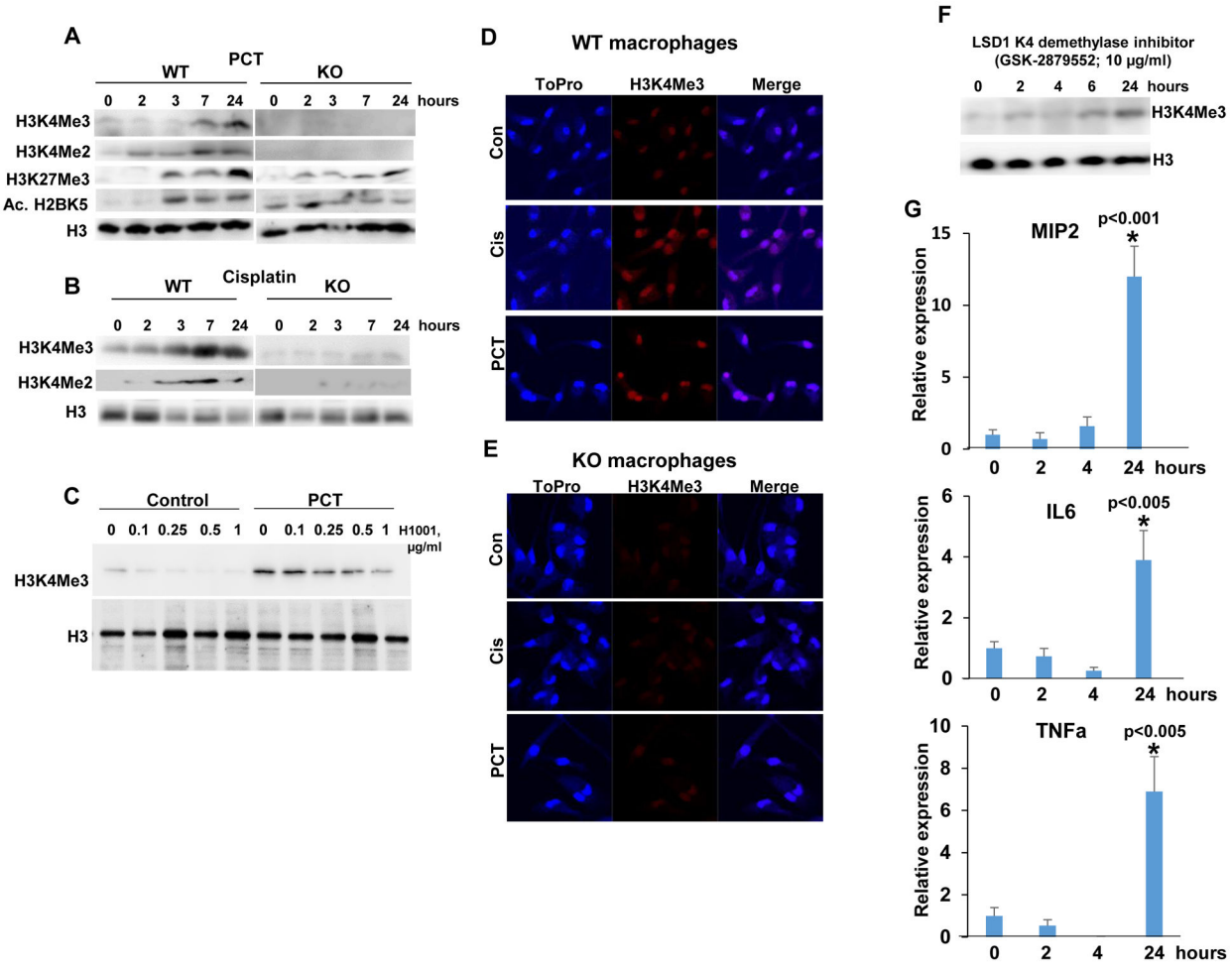

Figure 5.

PCT and cisplatin enhance H3K4 methylation. Peritoneal macrophages were isolated from WT and Hpa-KO mice and were left untreated (0) or were treated with PCT (15 μg/ml; **A**) and cisplatin (10 μg/ml; **B**) for the time indicated. Cell lysates were subjected to immunoblotting applying anti-tri- (Me3) and di- (Me2) methylated H3K4 (A, B upper and second panels), anti-tri-methylated H3K27 (A, third panels), anti-acetylated H2BK5 (A, fourth panels), and anti-H3 (A, B, lower panels) antibodies. Note that PCT and cisplatin markedly increase H3K4 methylation in WT but not Hpa-KO macrophages. **C**. Peritoneal macrophages were isolated from WT mice and were treated with PCT in the absence (0) or presence of the indicated concentrations of the heparanase inhibitor H1001. H1001 was also added to untreated macrophages (Control). DMSO was added as vehicle control (0). Cell lysates were prepared after 24 h and subjected to immunoblotting applying anti-tri-methylated H3K4 (upper panel) and anti-H3 (second panel) antibodies. **D**, **E**. Immunofluorescent staining. Peritoneal macrophages were isolated from WT (**D**) and Hpa-KO (**E**) mice and were left untreated (Con) or were treated with PCT (15 μg/ml) or cisplatin (10 μg/ml) for 24 h. Cells were then fixed and permeabilized with methanol for 20 min and subjected to immunofluorescent staining applying anti-tri-methylated H3K4 antibody (middle panels, red); Nuclear staining (ToPro) is shown in blue. Original magnifications:

x100. **F, G**. LSD1 inhibition results in increased cytokine expression. Peritoneal macrophages were isolated from WT mice and were left untreated (0) or were treated with GSK-2879552 (10 μg/ml), an inhibitor of the K4 de-methylate LSD1. DMSO was added as vehicle control (0). Cell lysates were prepared at the indicated times and subjected to immunoblotting applying anti-tri-methylated H3K4 (upper panel) and anti-H3 (lower panel) antibodies. Total RNA was extracted from corresponding macrophages cultures and was subjected to qPCR analyses applying primers specific for MIP2 (**G**, upper panel), IL6 (**G**, second panel), and TNFα (**G**, lower panel). *p<0.005 24 h vs. control (0).

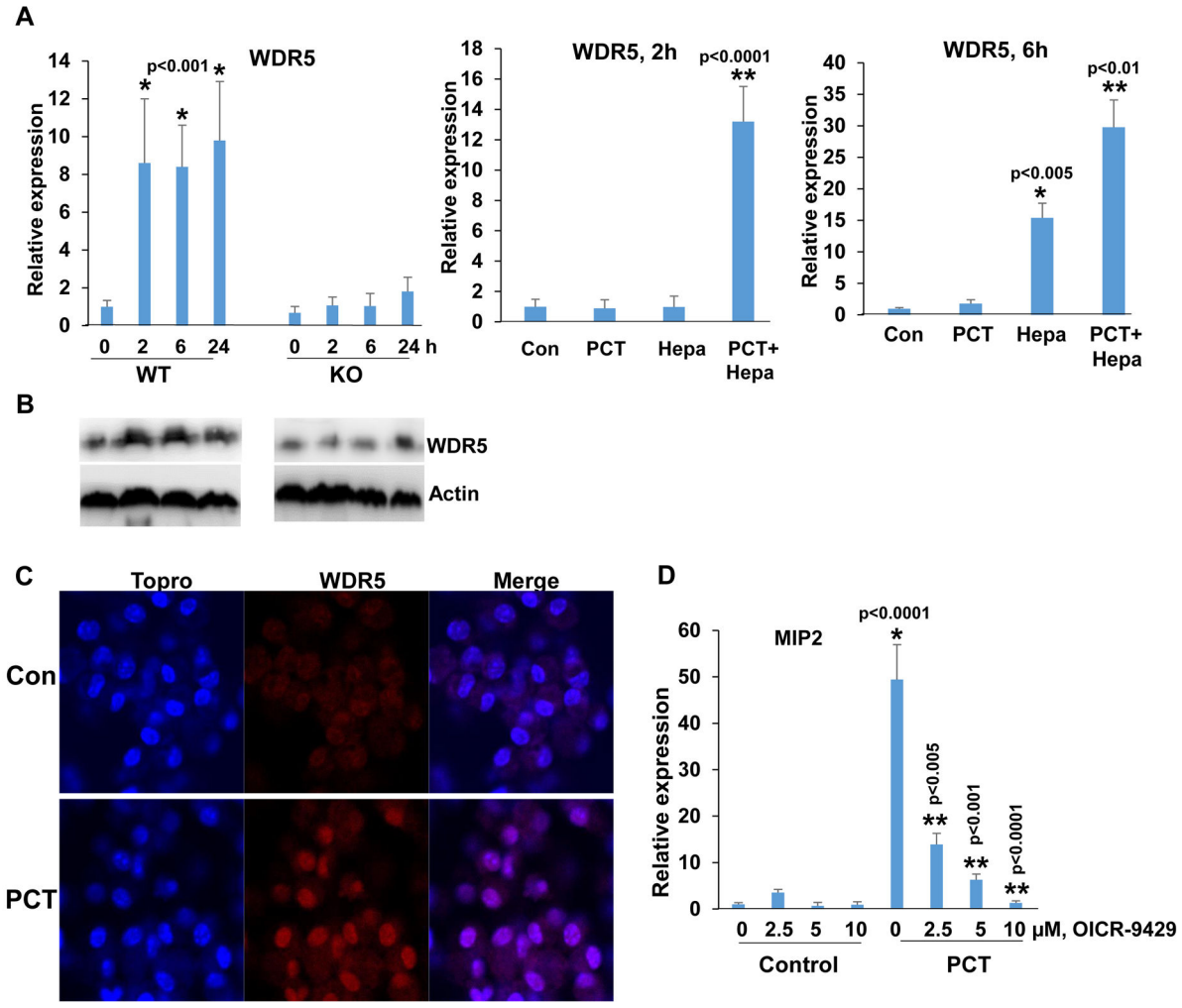

Figure 6.

WDR5 expression by PCT is heparanase-dependent. **A**. qPCR. Peritoneal macrophages were isolated from WT and Hpa-KO mice and were left untreated (0) or were treated with PCT (15 μg/ml) for the time indicated. Total RNA was then extracted and subjected to qPCR analysis applying primers specific for WDR5 (left panel). *p<0.001 vs control (0). Protein lysates were prepared from corresponding cultures and were subjected to immunoblotting applying anti-WDR5 (upper panels) and anti-actin (lower panels) antibodies (**B**). Hpa-KO macrophages were left untreated (Con) or were treated with PCT (15 μg/ml), heparanase (Hepa; 1 μg/ml), or both. Total RNA was extracted after 2 (A, middle panel) and 6 (A, right panel) hours, and WDR5 expression was quantified. *p<0.005 Hepa vs. Con; **p<0.01 PCT +Hepa vs Hepa. **C**. Immunofluorescent staining. Peritoneal macrophages were isolated from WT mice and were left untreated (Con) or were treated with PCT (15 μg/ml) for 24 h. Macrophages were then fixed and permeabilized with methanol, followed by immunofluorescent staining applying anti-WDR5 antibody (middle panels, red); Nuclear (ToPro) staining is shown in blue. **D**. Peritoneal macrophages were isolated from WT mice and were left untreated (Con) or were treated with PCT (15 μg/ml) in the absence (0) or the indicated concentrations of OICR-9429, a WDR5 inhibitor. DMSO was added as vehicle

control (0). Total RNA was extracted after 24 hours and was subjected to qPCR applying primers specific for MIP2. *p<0.001 PCT vs. Con;**p<0.005 PCT+OICR-9429 vs PCT.

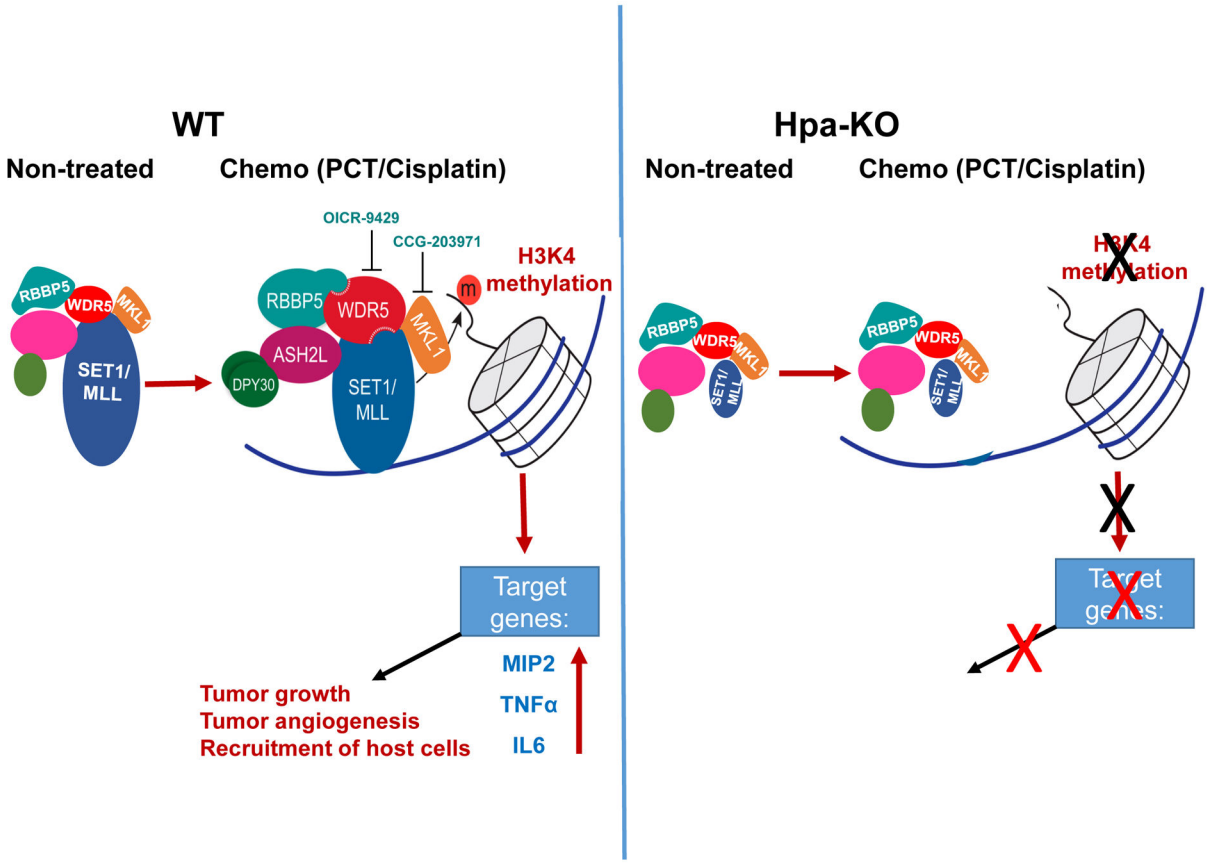

Figure 7.

A summary diagram of the results. In WT macrophages (left), treatment with PCT/Cisplatin induces the expression of WDR5 and MKL1, associating with increased H3K4 methylation, cytokine expression (i.e., MIP2) and tumor growth. Inhibition of WDR5 (OICR-9429) or MKL1 (CCG-203971) results in reduced cytokine expression. In Hpa-KO macrophages (right), the expression of SET1A, MLL1, and MKL1 are significantly lower vs. WT macrophages and their expression is not induced by PCT; H3K4 methylation is not increased by PCT/Cisplatin, nor cytokine expression.